2026 IEEE Intelligent Vehicles Symposium (IV)
June 22-25, 2026. Detroit, MI, USA

2026 IEEE Intelligent Vehicles Symposium (IV) | 979-8-3315-4793-6/26/$31.00 ©2026 IEEE | DOI: 10.1109/IV66570.2026.11623931

Safe Lane-Keeping with Lag-compensating Control Barrier Functions

Yuchen Chen, Illés Vörös, Tamas G. Molnar, and Gábor Orosz

***Abstract*— This paper presents a safety-critical lane-keeping controller for automated vehicles subject to actuator delay, modeled as a first-order lag. Such lags, arising from the steer-by-wire system, can significantly degrade safety but are often ignored in prior studies. To remedy this, we propose a *lag-compensating control barrier function* (LCCBF) by applying a state transformation to the CBF designed for the lag-free vehicle dynamics. Using LCCBF, we design a lag-aware safety filter that provides formal safety guarantees for lane keeping under lag. Comparative simulations demonstrate that, unlike high-order and backstepping CBFs, the proposed method features a simple formulation without additional parameters while consistently maintaining safety with less conservatism and control effort, ensuring robust and comfortable lane-keeping performance.**

I. Introduction

Automated vehicle (AV) technologies have advanced rapidly in recent years, promising substantial benefits such as improved passenger comfort, enhanced energy efficiency, and reduced traffic congestion. However, realizing these advantages in real-world deployment requires formally ensuring AV safety. Although modern AVs operate reliably across diverse scenarios using learning-based and data-driven algorithms [1], most of them still lack formal safety guarantees. In particular, they do not ensure that safety-critical requirements, such as lane keeping, are consistently satisfied.

To achieve safety, several approaches have been explored, such as model predictive control [2] and reachability analysis [3]. However, these methods often involve high computational complexity, making real-time, on-board implementation challenging. In contrast, control barrier functions (CBFs) [4] offer a computationally efficient framework with formal safety guarantees, enabling seamless integration into existing controllers as safety filters that prevent unsafe control actions. Owing to these advantages, CBF-based approaches have been applied in various driving scenarios, such as adaptive and connected cruise control [4], [5], emergency braking [6], and lane keeping [7], [8], [9], [10].

Time delays are inherent in AVs, arising from sensory data processing, state estimation, and actuator dynamics within the powertrain and steer-by-wire systems [11]. This may significantly compromise safety but is often neglected in prior studies. Time delays in vehicle dynamics are often approximated by first-order lags, which may help to simplify the design of controllers [12]. For such lagged systems, high-order CBFs (HOCBFs) [13] and backstepping CBFs (BSCBFs) [14] have been adopted to ensure safety, with applications in longitudinal control [15], [16]. However, HOCBFs may be invalid and fail to guarantee safety [17], while BSCBFs can be difficult to design and may lead to overly conservative vehicle behavior [16]. Besides, safe lane-keeping with lag is yet to be addressed.

Yuchen Chen, Illés Vörös, and Gábor Orosz are with the Department of Mechanical Engineering, University of Michigan, Ann Arbor, MI 48109, USA, {ethanch, illesvoe, orosz}@umich.edu.

Tamas G. Molnar is with the Department of Mechanical Engineering, Wichita State University, Wichita, KS 67260, USA, tamas.molnar@wichita.edu.

Gábor Orosz is also with the Department of Civil and Environmental Engineering, University of Michigan, Ann Arbor, MI 48109, USA.

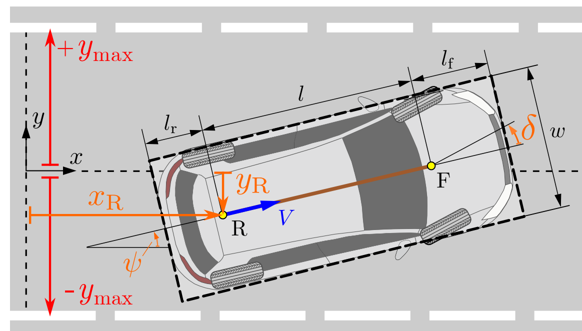

Fig. 1. Kinematic single-track vehicle model driving along a straight lane, extended with its bounding box.

In this paper, we apply the *lag-compensating control barrier function* (LCCBF) [18] to ensure safe lane-keeping for vehicles with first-order actuator lag. Specifically, we extend the CBF developed for the lag-free vehicle in [9] to offer provable safety guarantees for lagged vehicle dynamics without additional parameters. Using LCCBF, we design a lag-aware safety filter to minimally modify the desired but unsafe controllers to a safe one. Comparative analysis with BSCBF and HOCBF highlights that the proposed safety filter consistently ensures safety under lag with less control effort and conservatism.

The rest of the paper is organized as follows. Section II introduces the vehicle dynamics and the nominal controller for lane-keeping. Section III reviews the CBF theory and safety filter design for lag-free vehicle dynamics. Section IV proposes the novel LCCBF and the corresponding lag-aware safety filter, along with the comparative simulations with the BSCBF and HOCBF approaches. Section V concludes the paper and lays out future research directions.

II. Vehicle Model and Nominal Controller

We consider a kinematic single-track vehicle model illustrated in Fig. 1, where the tire slip is ignored and the longitudinal velocity $V > 0$ is assumed to be constant. The coordinates of the rear axle center R are denoted by $(x_{\rm R},\ y_{\rm R})$, while the yaw and steering angle are represented by ψ and δ, respectively. Besides, we enclose the vehicle by a bounding box defined by the wheelbase l, the front and rear overhangs $l_{\rm f} < l$ and $l_{\rm r} < l$, and the width w. Based on this, the governing equations are given by

$$\dot{x}_{\rm R} = V\cos\psi, \quad \dot{y}_{\rm R} = V\sin\psi, \quad \dot{\psi} = \frac{V}{l}\tan\delta. \tag{1}$$

The control input can be defined as the tangent of the steering angle, i.e., $u = \tan\delta$, which imposes a natural saturation on $\delta \in [-90°,\ 90°]$. Although this still allows large steering angles that are unrealistic for most passenger cars, it will be shown later that the steering commands generated by the proposed method stay inside the physically relevant range.

For simplicity, we assume that the vehicle travels in a straight lane aligned with the x-direction, such that the lane centerline coincides with the x-axis. The left and right lane boundaries are located at $y = y_{\max}$ and $y = -y_{\max}$; see the white dashed lines in Fig. 1. With this lane configuration, we can decouple the longitudinal dynamics, i.e., first equation in (1), in lane-keeping design. Since the yaw angle ψ in the lane is typically small, we apply the small angle approximation for ψ, i.e., $\sin\psi \approx \psi$. Then (1) becomes

$$\dot{y}_{\rm R} = V\psi, \quad \dot{\psi} = \frac{V}{l}u, \tag{2}$$

with the state $\mathbf{x} = [y_{\rm R}\ \ \psi]^\top$. If we incorporate the steering system response time as a first-order lag $\xi > 0$, we have

$$\dot{y}_{\rm R} = V\psi, \quad \dot{\psi} = \frac{V}{l}e, \quad \dot{e} = \frac{1}{\xi}(u - e), \tag{3}$$

with the lagged input e and the commanded control input u.

To stabilize the vehicle's motion along the x-axis, we design a nominal (or desired) state feedback controller:

$$u_{\rm d}(\mathbf{x}) = -P_y y_{\rm R} - P_\psi \psi, \tag{4}$$

where P_y and P_ψ are control gains selected via pole placement. Although $u_{\rm d}$ in (4) stabilizes the vehicle's straight-line motion, it offers no formal safety assurances for staying between the lane boundaries. To address this, we introduce a CBF-based safety filter that minimally modifies the nominal controller to ensure safe lane keeping, even under lag.

III. Safety Filter Without First-order Lag

This section reviews the background on CBFs and presents a safety filter for the lag-free vehicle (2) based on [9], [10].

A. Control barrier functions

Consider a single-input control-affine system:

$$\dot{\mathbf{x}} = \mathbf{f}(\mathbf{x}) + \mathbf{g}(\mathbf{x})u, \tag{5}$$

with state $\mathbf{x} \in \mathbb{R}^n$, input $u \in \mathbb{R}$, and locally Lipschitz continuous functions $\mathbf{f}, \mathbf{g} : \mathbb{R}^n \to \mathbb{R}^n$. Given an initial condition $\mathbf{x}(0) \in \mathbb{R}^n$, the system admits a unique solution $\mathbf{x}(t)$.

To characterize safety, we define the *safe set*:

$$\mathcal{S} = \{\mathbf{x} \in \mathbb{R}^n : h(\mathbf{x}) \geq 0\}, \tag{6}$$

where $h : \mathbb{R}^n \to \mathbb{R}$ is a continuously differentiable function. System (5) is safe w.r.t. $\mathcal{S}$ if $\mathcal{S}$ is forward invariant, i.e., $\mathbf{x}(0) \in \mathcal{S} \implies \mathbf{x}(t) \in \mathcal{S},\ \forall t \geq 0$. To enforce safety, control barrier functions (CBFs) [4] have been introduced.

Definition 1 ([4], [19])**.** Function $h : \mathbb{R}^n \to \mathbb{R}$ is a *control barrier function* for (5) on $\mathcal{S}$ if and only if for all $\mathbf{x} \in \mathcal{S}$:

$$\underbrace{\nabla h(\mathbf{x})\mathbf{g}(\mathbf{x})}_{L_{\mathbf{g}}h(\mathbf{x})} = 0 \implies \underbrace{\nabla h(\mathbf{x})\mathbf{f}(\mathbf{x})}_{L_{\mathbf{f}}h(\mathbf{x})} > -\alpha\big(h(\mathbf{x})\big). \tag{7}$$

Here $L_{\mathbf{f}}h$ and $L_{\mathbf{g}}h$ denote the Lie derivatives, and $\alpha \in \mathcal{K}^{\rm e}$ denotes an extended class-$\mathcal{K}$ function. For simplicity, we use the linear function $\alpha(r) = \gamma r$ with $\gamma > 0$ in this paper.

Theorem 1 ([4])**.** *If h is a CBF for (5) on $\mathcal{S}$, then any locally Lipschitz continuous controller $u(\mathbf{x})$ that satisfies:*

$$\dot{h}\big(\mathbf{x}, u(\mathbf{x})\big) = L_{\mathbf{f}}h(\mathbf{x}) + L_{\mathbf{g}}h(\mathbf{x})u(\mathbf{x}) \geq -\gamma h(\mathbf{x}), \tag{8}$$

for all $\mathbf{x} \in \mathcal{S}$ renders (5) safe w.r.t. $\mathcal{S}$.

One may design a safety filter that minimally adjusts the nominal controller $u_{\rm d}(\mathbf{x})$ subject to (8):

$$\begin{aligned} u(\mathbf{x}) = \underset{u \in \mathbb{R}}{\operatorname{argmin}}\ & \|u - u_{\rm d}(\mathbf{x})\|^2 \\ \text{s.t. } & \dot{h}(\mathbf{x}, u) \geq -\gamma h(\mathbf{x}). \end{aligned} \tag{9}$$

The analytical solution of (9) is given in [6] as

$$u(\mathbf{x}) = \begin{cases} \min\{u_{\rm d}(\mathbf{x}), u_{\rm s}(\mathbf{x})\}, & \text{if } L_{\mathbf{g}}h(\mathbf{x}) < 0, \\ u_{\rm d}(\mathbf{x}), & \text{if } L_{\mathbf{g}}h(\mathbf{x}) = 0, \\ \max\{u_{\rm d}(\mathbf{x}), u_{\rm s}(\mathbf{x})\}, & \text{if } L_{\mathbf{g}}h(\mathbf{x}) > 0, \end{cases} \tag{10}$$

with the safe controller

$$u_{\rm s}(\mathbf{x}) = -\frac{L_{\mathbf{f}}h(\mathbf{x}) + \gamma h(\mathbf{x})}{L_{\mathbf{g}}h(\mathbf{x})}. \tag{11}$$

B. Safety filter for lag-free vehicle dynamics

Based on (9), we design the safety filter for the lag-free vehicle model (2), rewritten in the control-affine form (5) as

$$\underbrace{\begin{bmatrix} \dot{y}_{\rm R} \\ \dot{\psi} \end{bmatrix}}_{\dot{\mathbf{x}}} = \underbrace{\begin{bmatrix} V\psi \\ 0 \end{bmatrix}}_{\mathbf{f}(\mathbf{x})} + \underbrace{\begin{bmatrix} 0 \\ \frac{V}{l} \end{bmatrix}}_{\mathbf{g}(\mathbf{x})} u. \tag{12}$$

The vehicle is considered safe if its bounding box remains entirely within the lane boundaries at all times; see Fig. 1. To ensure this, a valid CBF $h : \mathbb{R}^2 \to \mathbb{R}$ for (2) was proposed in [9] and experimentally validated in [10]:

$$h(\mathbf{x}) = a\psi^2 + b\psi y_{\rm R} + c y_{\rm R}^2 + d, \tag{13}$$

with the safe set $\mathcal{S} = \big\{\mathbf{x} \in \mathbb{R}^2 : h(\mathbf{x}) \geq 0\big\}$; see the green ellipse in Fig. 2(a). The parameters a, b, c, d are given by

$$\begin{aligned} a &= -1, \quad b = -\frac{2(l + l_{\rm f} + l_{\rm r})}{(l + l_{\rm f})^2 + l_{\rm r}^2}, \\ c &= -\frac{2}{(l + l_{\rm f})^2 + l_{\rm r}^2}, \quad d = \frac{(2y_{\max} - w)^2}{4\big((l + l_{\rm f})^2 + l_{\rm r}^2\big)}. \end{aligned} \tag{14}$$

Given $\nabla h(\mathbf{x}) = [b\psi + 2cy_{\rm R}\ \ 2a\psi + by_{\rm R}]$, we have

$$L_{\mathbf{f}}h(\mathbf{x}) = bV\psi^2 + 2cVy_{\rm R}\psi, \quad L_{\mathbf{g}}h(\mathbf{x}) = \frac{2aV\psi + bVy_{\rm R}}{l}. \tag{15}$$

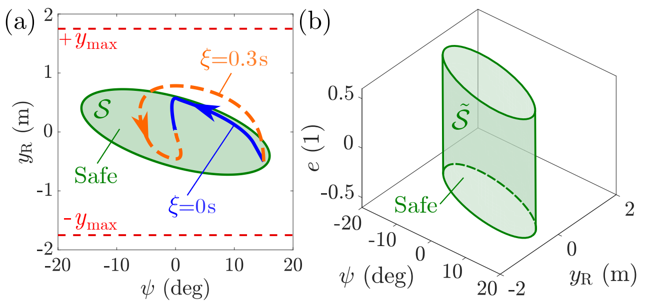

Fig. 2. (a) Safe set $\mathcal{S}$ defined by the CBF h in (13), and the simulations without lag (blue) and with lag (orange) using the lag-free safety filter (4), (16), (17); (b) safe set $\tilde{\mathcal{S}}$ defined by the lifted function $\tilde{h}$.

Then the safety filter can be derived from (10), (11), (15) as

$$u(\mathbf{x})=\begin{cases}\min\left\{u_{\mathrm{d}}(\mathbf{x}),u_{\mathrm{s}}(\mathbf{x})\right\}, & \text{if } y_{\mathrm{R}}>-\frac{2a}{b}\psi,\\ u_{\mathrm{d}}(\mathbf{x}), & \text{if } y_{\mathrm{R}}=-\frac{2a}{b}\psi,\\ \max\left\{u_{\mathrm{d}}(\mathbf{x}),u_{\mathrm{s}}(\mathbf{x})\right\}, & \text{if } y_{\mathrm{R}}<-\frac{2a}{b}\psi,\end{cases}\tag{16}$$

with the safe controller

$$u_{\mathrm{s}}(\mathbf{x})=-\frac{l\big(bV\psi^2+2cVy_{\mathrm{R}}\psi+\gamma h(\mathbf{x})\big)}{V(2a\psi+by_{\mathrm{R}})}.\tag{17}$$

Fig. 2(a) illustrates simulation results for the lag-free vehicle (2) and the lagged vehicle (3) with $\xi=0.3$ s. Both simulations use the lag-free safety filter (4), (16), (17) with parameters from Table I. The safety filter successfully maintains safety for the lag-free case, with the blue trajectory remaining inside the safe region (green); cf. [9]. However, it fails to ensure safety for the lag case, as the orange trajectory escapes the safe set. To overcome this, we introduce a novel lag-aware safety filter.

IV. Safety Filter With First-order Lag

In this section, we develop a lag-aware safety filter for the vehicle with first-order input lag (3). Specifically, we propose a *lag-compensating control barrier function* (LCCBF) based on the CBF (13). Compared with existing approaches such as the backstepping CBF [14] and the high-order CBF [13], the proposed LCCBF provides a parameter-free formulation while ensuring all-time safe and comfortable lane keeping.

We first rewrite (3) in the control-affine form:

$$\underbrace{\begin{bmatrix}\dot{y}_{\mathrm{R}}\\ \dot{\psi}\\ \dot{e}\end{bmatrix}}_{(\dot{\mathbf{x}},\dot{e})}=\underbrace{\begin{bmatrix}V\psi\\ \frac{V}{l}e\\ -\frac{1}{\xi}e\end{bmatrix}}_{\mathbf{F}(\mathbf{x},e)}+\underbrace{\begin{bmatrix}0\\0\\ \frac{1}{\xi}\end{bmatrix}}_{\mathbf{G}(\mathbf{x},e)}u.\tag{18}$$

We then lift the CBF h in (13) to the augmented space $(\mathbf{x},e)$ and define $\tilde{h}:\mathbb{R}^3\to\mathbb{R}$ as $\tilde{h}(\mathbf{x},e)\triangleq h(\mathbf{x})$, with the corresponding set $\tilde{\mathcal{S}}=\{(\mathbf{x},e)\in\mathbb{R}^3:\tilde{h}(\mathbf{x},e)\geq 0\}=\mathcal{S}\times\mathbb{R}$; see Fig. 2(b). From (13), (15) and (18), we obtain:

$$L_{\mathbf{G}}\tilde{h}(\mathbf{x},e)=0,\quad L_{\mathbf{F}}\tilde{h}(\mathbf{x},e)=L_{\mathbf{f}}h(\mathbf{x})+L_{\mathbf{g}}h(\mathbf{x})e,\tag{19}$$

for all $(\mathbf{x},e)\in\tilde{\mathcal{S}}$. This implies that the control input u does not influence the safety condition (8). Moreover, there exists $\mathbf{x}$ and e such that $L_{\mathbf{F}}\tilde{h}(\mathbf{x},e)>-\alpha\big(\tilde{h}(\mathbf{x},e)\big)$ does not hold. Hence, by (7), $\tilde{h}$ is not a valid CBF and fails to ensure the safety of (18), as shown by the orange trajectory in Fig. 2(a).

TABLE I

Parameters of the Simulations

Category	Variable	Symbol	Value	Unit
Vehicle	wheelbase	l	2.7	m
	overhangs	$(l_{\mathrm{f}},l_{\mathrm{r}})$	$(0.9,0.7)$	m
	width	w	1.8	m
	longitudinal velocity	V	10	m/s
	first-order lag	ξ	0.3	s
Lane	lane boundary	$y_{\max}$	1.75	m
CBFs	class-$\mathcal{K}$ function	$(\gamma,\gamma_{\mathrm{ho}})$	$(1,1)$	1/s
	BSCBF parameter	μ	1	1
	BSCBF gains	(k_y,k_ψ)	$(0.8,2)$	$(1/\mathrm{m},1)$
Controller	stable gains	(P_y,P_ψ)	$(0.007,0.27)$	$(1/\mathrm{m},1)$

To remedy this, we introduce the LCCBF $h_{\mathrm{lc}}:\mathbb{R}^3\to\mathbb{R}$ first proposed in [18]. First, we define the state transformation

$$\hat{\mathbf{x}}=\mathbf{x}+\xi\dot{\mathbf{x}}\quad\Leftrightarrow\quad\begin{bmatrix}\hat{y}_{\mathrm{R}}\\ \hat{\psi}\end{bmatrix}=\begin{bmatrix}y_{\mathrm{R}}+\xi V\psi\\ \psi+\frac{\xi V}{l}e\end{bmatrix}.\tag{20}$$

Here $\hat{\mathbf{x}}$ can be viewed as a prediction of the future state as it yields the corresponding lag-free dynamics:

$$\dot{\hat{\mathbf{x}}}=\begin{bmatrix}\dot{y}_{\mathrm{R}}+\xi V\dot{\psi}\\ \dot{\psi}+\frac{\xi V}{l}\dot{e}\end{bmatrix}=\begin{bmatrix}V\hat{\psi}\\ \frac{V}{l}u\end{bmatrix}=\mathbf{f}(\hat{\mathbf{x}})+\mathbf{g}(\hat{\mathbf{x}})u.\tag{21}$$

By (20), the LCCBF candidate is constructed from (13) as:

$$\begin{aligned}h_{\mathrm{lc}}(\mathbf{x},e)=&h(\hat{\mathbf{x}})=a\hat{\psi}^2+b\hat{\psi}\hat{y}_{\mathrm{R}}+c\hat{y}_{\mathrm{R}}^2+d\\ =&a\big(\psi+\tfrac{\xi V}{l}e\big)^2+b\big(\psi+\tfrac{\xi V}{l}e\big)\big(y_{\mathrm{R}}+\xi V\psi\big)\\ &+c\big(y_{\mathrm{R}}+\xi V\psi\big)^2+d,\end{aligned}\tag{22}$$

with the safe set $\mathcal{S}_{\mathrm{lc}}=\{(\mathbf{x},e)\in\mathbb{R}^3:h_{\mathrm{lc}}(\mathbf{x},e)\geq 0\}$. From (18), (22), the Lie derivatives of h_{lc} are:

$$\begin{aligned}L_{\mathbf{F}}h_{\mathrm{lc}}(\mathbf{x},e)&=bV\hat{\psi}^2+2cV\hat{y}_{\mathrm{R}}\hat{\psi}=L_{\mathbf{f}}h(\hat{\mathbf{x}}),\\ L_{\mathbf{G}}h_{\mathrm{lc}}(\mathbf{x},e)&=\frac{2aV\hat{\psi}+bV\hat{y}_{\mathrm{R}}}{l}=L_{\mathbf{g}}h(\hat{\mathbf{x}}).\end{aligned}\tag{23}$$

By (10), (11), (23), the lag-aware safety filter u_{lc} is:

$$u_{\mathrm{lc}}(\mathbf{x},e)=\begin{cases}\min\left\{u_{\mathrm{d}}(\mathbf{x}),u_{\mathrm{s}}^{\mathrm{lc}}(\mathbf{x},e)\right\}, & \text{if } \hat{y}_{\mathrm{R}}>-\frac{2a}{b}\hat{\psi},\\ u_{\mathrm{d}}(\mathbf{x}), & \text{if } \hat{y}_{\mathrm{R}}=-\frac{2a}{b}\hat{\psi},\\ \max\left\{u_{\mathrm{d}}(\mathbf{x}),u_{\mathrm{s}}^{\mathrm{lc}}(\mathbf{x},e)\right\}, & \text{if } \hat{y}_{\mathrm{R}}<-\frac{2a}{b}\hat{\psi},\end{cases}\tag{24}$$

with the safe controller

$$u_{\mathrm{s}}^{\mathrm{lc}}(\mathbf{x},e)=-\frac{l\big(bV\hat{\psi}^2+2cV\hat{y}_{\mathrm{R}}\hat{\psi}+\gamma h_{\mathrm{lc}}(\mathbf{x},e)\big)}{V(2a\hat{\psi}+b\hat{y}_{\mathrm{R}})}.\tag{25}$$

Note that $u_{\mathrm{s}}^{\mathrm{lc}}$ can be derived by substituting $\hat{\mathbf{x}}$ from (20) into the lag-free safe controller u_{s} in (17), i.e., $u_{\mathrm{s}}^{\mathrm{lc}}(\mathbf{x},e)\triangleq u_{\mathrm{s}}(\hat{\mathbf{x}})$. Although (25) is singular when $\hat{y}_{\mathrm{R}}=-\frac{2a}{b}\hat{\psi}$, (24) ensures that only u_{d} is active in this region, keeping u_{lc} well-defined. The following theorem establishes that the LCCBF-based safety filter (24), (25) ensures safe lane keeping for (18).

Theorem 2. The LCCBF candidate h_{lc} in (22) is a valid CBF for (18) on $\mathcal{S}_{\mathrm{lc}}$. Moreover, the lag-aware safety filter u_{lc} in (24), (25) renders (18) safe w.r.t. $\mathcal{S}_{\mathrm{lc}}\cap\tilde{\mathcal{S}}$.

Please refer to the Appendix for the proof of Theorem 2.

We compare the proposed safe lane-keeping controller to two baseline methods. The first baseline approach is to construct a *backstepping CBF* (BSCBF) [14], defined as:

$$\begin{aligned} h_{\rm bs}(\mathbf{x}, e) &= h(\mathbf{x}) - \frac{\big(e - u_v(\mathbf{x})\big)^2}{2\mu} \\ &= a\psi^2 + b\psi y_{\rm R} + c y_{\rm R}^2 + d - \frac{(e + k_y y_{\rm R} + k_\psi \psi)^2}{2\mu}, \end{aligned} \tag{26}$$

with parameter $\mu > 0$ and the corresponding safe set $\mathcal{S}_{\rm bs} = \{(\mathbf{x}, e) \in \mathbb{R}^3 : h_{\rm bs}(\mathbf{x}, e) \geq 0\}$. This involves designing a safe virtual controller u_v that satisfies the CBF condition (8) for the lag-free dynamics (12) on $\mathcal{S}$. Here we adopt a simple state feedback controller $u_v(\mathbf{x}) = -k_y y_{\rm R} - k_\psi \psi$ that can be shown to be safe with appropriate gains (k_y, k_ψ) [20].

From (18), (26), the Lie derivatives of $h_{\rm bs}$ are

$$\begin{aligned} L_{\mathbf{G}} h_{\rm bs}(\mathbf{x}, e) &= -\frac{1}{\xi}\frac{e + k_y y_{\rm R} + k_\psi \psi}{\mu} = -\frac{1}{\xi}\eta, \end{aligned} \tag{27}$$

$$L_{\mathbf{F}} h_{\rm bs}(\mathbf{x}, e) = L_{\mathbf{f}} h(\mathbf{x}) + L_{\mathbf{g}} h(\mathbf{x}) e - \eta V \left(k_y \psi + \frac{k_\psi e}{l} - \frac{e}{V\xi}\right),$$

which, when substituted into (10) and (11), yield the BSCBF-based safety filter $u_{\rm bs}(\mathbf{x}, e)$ with the safe controller $u_{\rm s}^{\rm bs}(\mathbf{x}, e)$. According to [14], $u_{\rm bs}$ ensures the safety of (18) w.r.t. $\mathcal{S}_{\rm bs}$.

The second baseline is the *high-order CBF* (HOCBF) [13]:

$$\begin{aligned} h_{\rm ho}(\mathbf{x}, e) &= L_{\mathbf{F}} \tilde{h}(\mathbf{x}, e) + \gamma_{\rm ho} \tilde{h}(\mathbf{x}, e) \\ &= L_{\mathbf{f}} h(\mathbf{x}) + L_{\mathbf{g}} h(\mathbf{x}) e + \gamma_{\rm ho} h(\mathbf{x}), \end{aligned} \tag{28}$$

with parameter $\gamma_{\rm ho} > 0$ and the corresponding safe set $\mathcal{S}_{\rm ho} = \{(\mathbf{x}, e) \in \mathbb{R}^3 : h_{\rm ho}(\mathbf{x}, e) \geq 0\}$.

By (18), (28), the Lie derivatives of $h_{\rm ho}$ are

$$\begin{aligned} L_{\mathbf{G}} h_{\rm ho}(\mathbf{x}, e) &= L_{\mathbf{g}} h(\mathbf{x})/\xi, \\ L_{\mathbf{F}} h_{\rm ho}(\mathbf{x}, e) &= \gamma_{\rm ho}\big(L_{\mathbf{f}} h(\mathbf{x}) + L_{\mathbf{g}} h(\mathbf{x}) e\big) - L_{\mathbf{g}} h(\mathbf{x}) e/\xi \\ &\quad + 2cV^2\psi^2 + \frac{3bV^2}{l}\psi e + \frac{2cV^2}{l} y_{\rm R} e + \frac{2aV^2}{l^2} e^2. \end{aligned} \tag{29}$$

Following [13], the safety of (18) can be enforced on $\mathcal{S}_{\rm ho} \cap \tilde{\mathcal{S}}$ using the HOCBF-based safety filter $u_{\rm ho}(\mathbf{x}, e)$ with the safe controller $u_{\rm s}^{\rm ho}(\mathbf{x}, e)$, obtained by substituting (29) into (10), (11). However, when $y_{\rm R} = \psi = 0$, we have $L_{\mathbf{g}} h(\mathbf{x}) = L_{\mathbf{f}} h(\mathbf{x}) = 0$, yielding

$$\begin{aligned} &L_{\mathbf{G}} h_{\rm ho}(\mathbf{x}, e) = 0, \quad L_{\mathbf{F}} h_{\rm ho}(\mathbf{x}, e) = \frac{2aV^2}{l^2} e^2, \\ &h_{\rm ho}(\mathbf{x}, e) = \gamma_{\rm ho} d > 0. \end{aligned} \tag{30}$$

Since $a < 0$, there exists a large e such that $(\mathbf{x}, e) \in \mathcal{S}_{\rm ho} \cap \tilde{\mathcal{S}}$ and $L_{\mathbf{F}} h_{\rm ho}(\mathbf{x}, e) < -\gamma h_{\rm ho}(\mathbf{x}, e)$ which violates (7). Therefore, $h_{\rm ho}$ in (28) is not a valid CBF. Moreover, the safety filter (10) becomes singular, as we have:

$$\lim_{\mathbf{x} \to \mathbf{0}} u_{\rm ho}(\mathbf{x}, e) = \begin{cases} -\infty, & \text{if } L_{\mathbf{G}} h_{\rm ho}(\mathbf{x}, e) \to 0^-, \\ +\infty, & \text{if } L_{\mathbf{G}} h_{\rm ho}(\mathbf{x}, e) \to 0^+, \end{cases} \tag{31}$$

when $L_{\mathbf{F}} h_{\rm ho}(\mathbf{x}, e) < -\gamma h_{\rm ho}(\mathbf{x}, e)$. Therefore, $u_{\rm ho}$ is infeasible and cannot guarantee safe lane keeping.

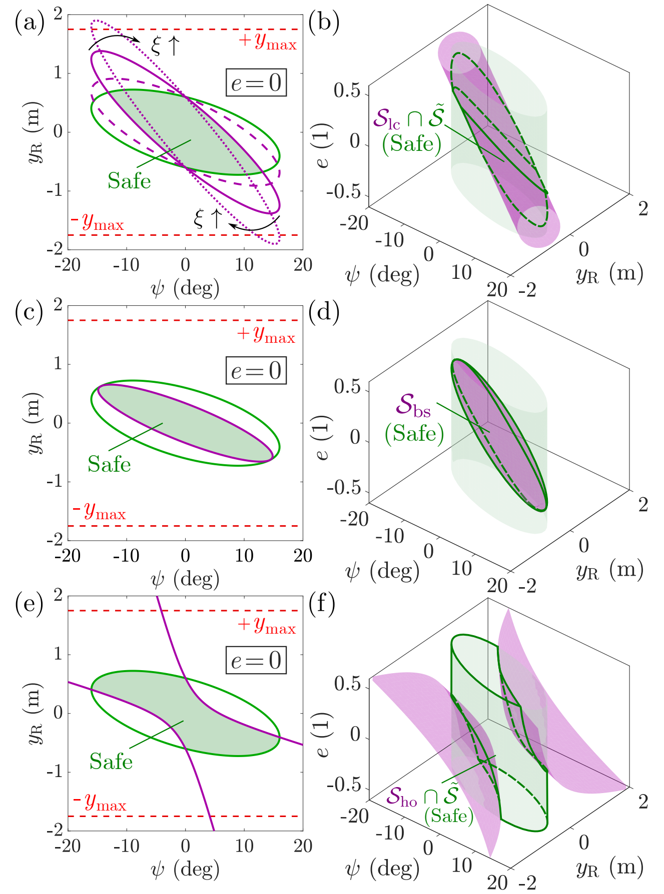

Fig. 3. Safe sets for lane keeping with lag: (a,b) $\mathcal{S}_{\rm lc}$ from LCCBF (22); (c,d) $\mathcal{S}_{\rm bs}$ from BSCBF (26); and (e,f) $\mathcal{S}_{\rm ho}$ from HOCBF (28). The nominal set $\tilde{\mathcal{S}}$ (green) and extended sets (purple) illustrate the regions for which (18) is rendered safe. Panels (a,c,e) show the section of (b,d,f) where $e = 0$.

Fig. 3 compares the three above-described methods for lane keeping. The set $\tilde{\mathcal{S}}$ (green ellipse) captures the safety constraint, i.e., keeping the vehicle in the lane, as given by the lifted function $\tilde{h}$. The purple sets illustrate the extended safe sets $\mathcal{S}_{\rm lc}$, $\mathcal{S}_{\rm bs}$, and $\mathcal{S}_{\rm ho}$ defined by the LCCBF (22), BSCBF (26), and HOCBF (28), respectively. The sets are visualized in both the $(\psi, y_{\rm R})$ and $(\psi, y_{\rm R}, e)$ spaces using the parameters in Table I. The green regions in Fig. 3(a,c,e) and their outlines in Fig. 3(b,d,f) indicate the safe domains of vehicle (18), namely $\mathcal{S}_{\rm lc} \cap \tilde{\mathcal{S}}$, $\mathcal{S}_{\rm bs}$, and $\mathcal{S}_{\rm ho} \cap \tilde{\mathcal{S}}$. The corresponding safety filters seek to keep the vehicle's lateral position and yaw angle inside these regions. All three regions are smaller than the set $\tilde{\mathcal{S}}$, reflecting the adverse impact of lag on safety. As the lag ξ increases, the LCCBF safe set $\mathcal{S}_{\rm lc}$ rotates clockwise and stretches, further shrinking the safe region $\mathcal{S}_{\rm lc} \cap \tilde{\mathcal{S}}$; see Fig. 3(a). Conversely, the BSCBF and HOCBF safe sets remain unchanged; see Fig. 3(c,e). The BSCBF yields the most conservative safe region, while the HOCBF allows unbounded e values; see Fig. 3(d,f). However, the HOCBF is not a valid CBF and leads to a singular safety filter as was proven above.

We simulate a vehicle with lag (18) using the LCCBF-based safety filter $u_{\rm lc}$ (4), (24), (25); see Fig. 4(a,d,e). For comparison, the BSCBF-based and HOCBF-based safety filters $u_{\rm bs}$ and $u_{\rm ho}$ are also simulated for the same vehicle, see

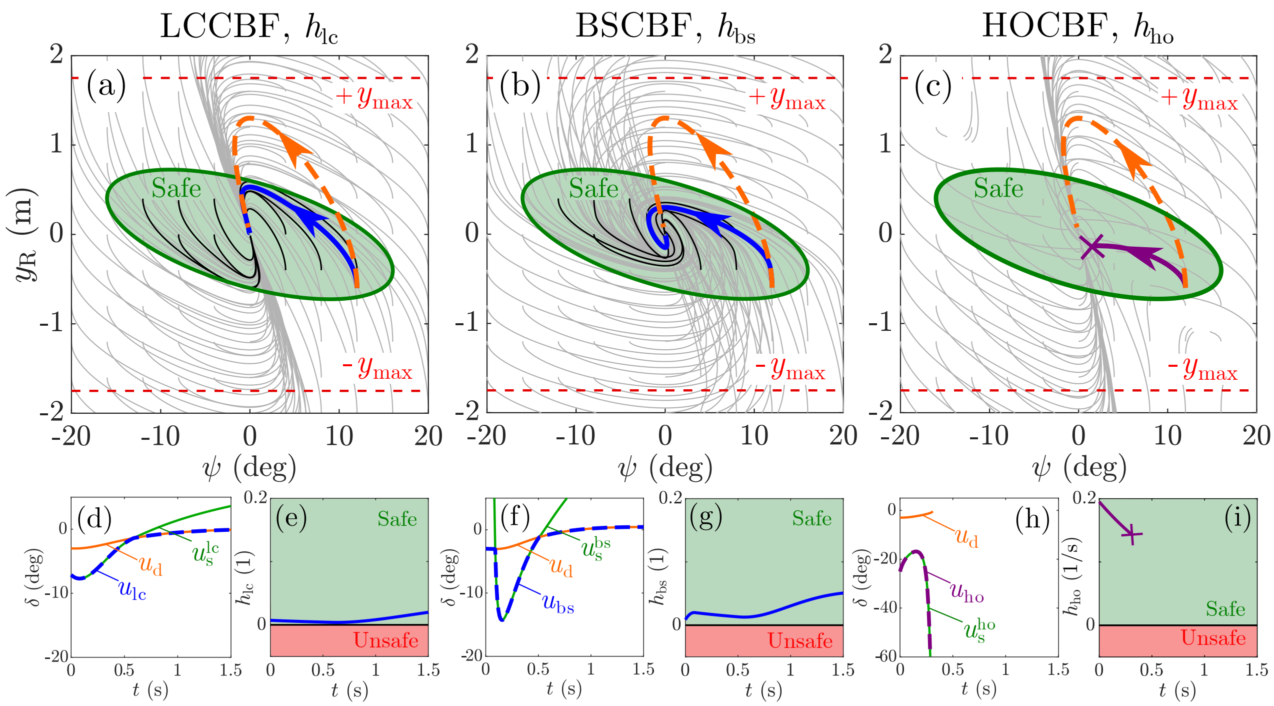

Fig. 4. Simulations of the vehicle with first-order lag (18). (a-c) State trajectories using the safety filters (gray, black, blue, purple) derived by LCCBF (22), BSCBF (26), and HOCBF (28), respectively, and using only the nominal controller (orange) from (4). (d,f,h) Steering angle δ for the blue and purple curves in (a-c), driven by the nominal controllers (orange), safe controllers (green) and safety filters (blue, purple). (e,g,i) CBF values $h_{\rm lc}$, $h_{\rm bs}$, and $h_{\rm ho}$ for the blue and purple curves in (a-c). Note that cross marks indicate that the simulation stops due to singularity.

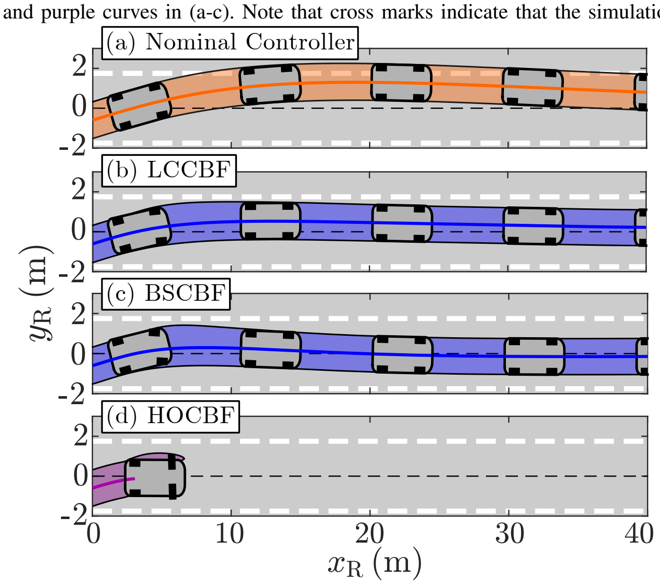

Fig. 5. Simulated vehicle trajectories using (a) nominal controller only, and safety filters based on (b) LCCBF, (c) BSCBF, and (d) HOCBF. The colored curves depict the motion of the rear-axle center.

Fig. 4(b,f,g) and Fig. 4(c,h,i), respectively. All simulations use the parameters in Table I.

Fig. 4(a,b) shows that both the LCCBF- and BSCBF-based safety filters successfully maintain safety, as the blue and black trajectories start and remain within the safe domain, while the nominal controller (orange) fails to do so. For trajectories that start outside the safe domain (gray), both safety filters render the safe set attractive. The nonnegative values of $h_{\rm lc}$ and $h_{\rm bs}$ in Fig. 4(e,g) further confirm safety w.r.t. the extended sets $\mathcal{S}_{\rm lc}$ and $\mathcal{S}_{\rm bs}$. Compared with BSCBF, the LCCBF achieves safety with less conservatism and a smaller steering angle; see the blue curves in Fig. 4(a,b,d,f). This improvement arises because the BSCBF (26) requires a safe virtual controller u_v, which is often nontrivial to design and can introduce unnecessary conservatism. Conversely, the LCCBF compensates for actuator lag by predicting and safeguarding future states, eliminating the need for complicated parameter tuning and avoiding additional conservatism. For the HOCBF, the safety filter becomes singular, as shown in Fig. 4(h), making safe lane-keeping infeasible.

Fig. 5 illustrates the vehicle trajectories in the $(x_{\rm R}, y_{\rm R})$ plane for different controllers. The colored curves represent the motion of the rear-axle center, corresponding to the nominal and safety-filtered trajectories with the same colors in Fig. 4(a–c). The nominal controller in Fig. 5(a) fails to keep the vehicle within the lane boundaries, while the safety filters in Fig. 5(b,c) successfully maintain lane keeping. Notably, the HOCBF-based filter gets stuck in Fig. 5(d) due to its singular input, causing an unrealistically large steering angle. Compared with the BSCBF-based filter in Fig. 5(c), the proposed LCCBF-based filter in Fig. 5(b) achieves less abrupt steering, as shown in Fig. 4(d,f), and gently guides the vehicle back to the lane center, ensuring both safety and passenger comfort.

V. Conclusion

In this paper, we proposed a safety-critical lane-keeping controller for automated vehicles with actuator lag. We introduced a lag-compensating control barrier function (LCCBF) that extends the formal safety assurance of the lag-free vehicle dynamics to those with lag, while retaining a simple formulation without additional parameters. Based on the LCCBF, a lag-aware safety filter was developed to modify unsafe actions from the nominal controller in a minimally invasive manner. Comparative simulations demonstrated that, unlike backstepping and high-order CBF-based methods, the proposed LCCBF approach consistently ensures safe lane-keeping with smaller steering angle and reduced conservatism, achieving both safety and passenger comfort. Future work will extend the framework to more sophisticated vehicle models and driving scenarios, such as curved roads.

APPENDIX

Proof of Theorem 2. We first show that $h_{\rm lc}$ is a valid CBF for (18) on $\mathcal{S}_{\rm lc}$ by verifying that (7) holds. By (23), $L_{\mathbf{G}} h_{\rm lc}(\mathbf{x}, e) = 0$ if and only if $\hat{y}_{\rm R} = -2a\hat{\psi}/b$. Substituting this into $L_{\mathbf{F}} h_{\rm lc}(\mathbf{x}, e)$ in (23) yields:

$$L_{\mathbf{F}} h_{\rm lc}(\mathbf{x}, e) = \left(b - \frac{4ac}{b}\right) V \hat{\psi}^2. \tag{32}$$

Using (14) and the geometric condition $l + l_{\rm f} > l_{\rm r}$, one may show that

$$b - \frac{4ac}{b} = \frac{2(l + l_{\rm f} + l_{\rm r})^2}{\big((l + l_{\rm f})^2 + l_{\rm r}^2\big)(l + l_{\rm f} - l_{\rm r})} > 0. \tag{33}$$

Hence, $L_{\mathbf{F}} h_{\rm lc}(\mathbf{x}, e) \geq 0$ for all $(\mathbf{x}, e) \in \mathcal{S}_{\rm lc}$, and equality holds if and only if $\hat{\psi} = \hat{y}_{\rm R} = 0$. Moreover, for any $\alpha \in \mathcal{K}^{\rm e}$, we have $-\alpha\big(h_{\rm lc}(\mathbf{x}, e)\big) \leq 0$ for all $(\mathbf{x}, e) \in \mathcal{S}_{\rm lc}$, and $-\alpha\big(h_{\rm lc}(\mathbf{x}, e)\big) = -\alpha(d) < 0$ when $\hat{\psi} = \hat{y_{\rm R}} = 0$. Therefore, (7) holds, and $h_{\rm lc}$ is a valid CBF for (18) on $\mathcal{S}_{\rm lc}$.

Next, we show that $u_{\rm lc}$ in (24) renders (18) safe w.r.t. $\mathcal{S}_{\rm lc} \cap \tilde{\mathcal{S}}$ using Theorem 1 on $\mathcal{S}_{\rm lc}$ and $\tilde{\mathcal{S}}$, respectively. From the construction of safety filter (9) we have

$$L_{\mathbf{F}} h_{\rm lc}(\mathbf{x}, e) + L_{\mathbf{G}} h_{\rm lc}(\mathbf{x}, e) u_{\rm lc}(\mathbf{x}, e) \geq -\gamma h_{\rm lc}(\mathbf{x}, e), \tag{34}$$

cf. (8). Therefore, Theorem 1 holds for (18) w.r.t. $\mathcal{S}_{\rm lc}$. For $\tilde{\mathcal{S}}$, safety is guaranteed if there exists a $\gamma > 0$ such that

$$\dot{\tilde{h}}\big(\mathbf{x}, e, u_{\rm lc}(\mathbf{x}, e)\big) \geq -\gamma \tilde{h}(\mathbf{x}, e), \tag{35}$$

for all $(\mathbf{x}, e) \in \mathcal{S}_{\rm lc} \cap \tilde{\mathcal{S}}$ based on Theorem 1. Applying a second-order Taylor expansion with the mean-value theorem to the LCCBF (22) yields

$$\begin{aligned} h_{\rm lc}(\mathbf{x}, e) &= h(\hat{\mathbf{x}}) = h(\mathbf{x} + \xi \dot{\mathbf{x}}) \\ &= h(\mathbf{x}) + \xi \nabla h(\mathbf{x}) \dot{\mathbf{x}} + \tfrac{\xi^2}{2} \dot{\mathbf{x}}^\top \nabla^2 h(\mathbf{x} + s\dot{\mathbf{x}}) \dot{\mathbf{x}}, \end{aligned} \tag{36}$$

for some $s \in [0, \xi]$ and all $(\mathbf{x}, e) \in \mathcal{S}_{\rm lc} \cap \tilde{\mathcal{S}}$. Since $a, b, c < 0$ in (14) and $4ac > b^2$ from (33), we have

$$\nabla^2 h(\mathbf{x} + s\dot{\mathbf{x}}) = \begin{bmatrix} 2c & b \\ b & 2a \end{bmatrix} \prec 0, \tag{37}$$

thus h is globally concave and $h_{\rm lc}(\mathbf{x}, e) \leq h(\mathbf{x}) + \xi \nabla h(\mathbf{x}) \dot{\mathbf{x}}$.

As $L_{\mathbf{G}} \tilde{h}(\mathbf{x}, e) = 0$ in (19), the lifted function $\tilde{h}$ satisfies

$$\dot{\tilde{h}}\big(\mathbf{x}, e, u_{\rm lc}(\mathbf{x}, e)\big) = L_{\mathbf{F}} \tilde{h}(\mathbf{x}, e) = \nabla h(\mathbf{x}) \dot{\mathbf{x}}. \tag{38}$$

Since $\tilde{h}(\mathbf{x}, e) = h(\mathbf{x})$, substituting (38) into (36) yields

$$\dot{\tilde{h}}\big(\mathbf{x}, e, u_{\rm lc}(\mathbf{x}, e)\big) \geq \frac{1}{\xi}\big(h_{\rm lc}(\mathbf{x}, e) - \tilde{h}(\mathbf{x}, e)\big). \tag{39}$$

Since $h_{\rm lc}(\mathbf{x}, e) \geq 0$ for all $(\mathbf{x}, e) \in \mathcal{S}_{\rm lc} \cap \tilde{\mathcal{S}}$, (39) implies (35) with $\gamma = 1/\xi$. Therefore, the safety of (18) is established w.r.t. $\mathcal{S}_{\rm lc} \cap \tilde{\mathcal{S}}$, completing the proof. □

REFERENCES

[1] U. Rosolia, X. Zhang, and F. Borrelli, "Data-driven predictive control for autonomous systems," *Annual Review of Control, Robotics, and Autonomous Systems*, vol. 1, no. 1, pp. 259–286, 2018.

[2] C. Massera Filho, M. H. Terra, and D. F. Wolf, "Safe optimization of highway traffic with robust model predictive control-based cooperative adaptive cruise control," *IEEE Transactions on Intelligent Transportation Systems*, vol. 18, no. 11, pp. 3193–3203, 2017.

[3] M. Chen, S. L. Herbert, H. Hu, Y. Pu, J. F. Fisac, S. Bansal, S. Han, and C. J. Tomlin, "FaSTrack: A modular framework for real-time motion planning and guaranteed safe tracking," *IEEE Transactions on Automatic Control*, vol. 66, no. 12, pp. 5861–5876, 2021.

[4] A. D. Ames, X. Xu, J. W. Grizzle, and P. Tabuada, "Control barrier function based quadratic programs for safety critical systems," *IEEE Transactions on Automatic Control*, vol. 62, no. 8, pp. 3861–3876, 2017.

[5] Y. Chen, T. G. Molnar, and G. Orosz, "Safety-critical connected cruise control: Leveraging connectivity for safe and efficient longitudinal control of automated vehicles," in *27th IEEE International Conference on Intelligent Transportation Systems*, 2024, pp. 110–115.

[6] A. Alan, A. J. Taylor, C. R. He, A. D. Ames, and G. Orosz, "Control barrier functions and input-to-state safety with application to automated vehicles," *IEEE Transactions on Control Systems Technology*, vol. 31, no. 6, pp. 2744–2759, 2023.

[7] X. Xu, J. W. Grizzle, P. Tabuada, and A. D. Ames, "Correctness guarantees for the composition of lane keeping and adaptive cruise control," *IEEE Transactions on Automation Science and Engineering*, vol. 15, no. 3, pp. 1216–1229, 2018.

[8] S. Brüggemann, D. Steeves, and M. Krstic, "Simultaneous lane-keeping and obstacle avoidance by combining model predictive control and control barrier functions," in *61st IEEE Conference on Decision and Control*, 2022, pp. 5285–5290.

[9] C. Jiang, H. Gan, I. Vörös, D. Takács, and G. Orosz, "Safety filter for lane-keeping control," in *16th International Symposium on Advanced Vehicle Control*, 2024, pp. 371–377.

[10] I. Vörös, X. Li, I. Kolmanovsky, J. Talbot, J. Dallas, M. Suminaka, J. Subosits, and G. Orosz, "Lane-keeping guardian with safety filter: Experimental validation," in *36th IEEE Intelligent Vehicles Symposium*, 2025, pp. 1490–1495.

[11] S. Beregi, S. S. Avedisov, C. R. He, D. Takács, and G. Orosz, "Connectivity-based delay-tolerant control of automated vehicles: theory and experiments," *IEEE Transactions on Intelligent Vehicles*, vol. 8, no. 1, pp. 275–289, 2023.

[12] G. Orosz and T. G. Molnár, *Dynamics and Control of Connected Vehicles*. Springer, 2025.

[13] W. Xiao and C. Belta, "Control barrier functions for systems with high relative degree," in *58th IEEE Conference on Decision and Control*, 2019, pp. 474–479.

[14] A. J. Taylor, P. Ong, T. G. Molnar, and A. D. Ames, "Safe backstepping with control barrier functions," in *61st IEEE Conference on Decision and Control*, 2022, pp. 5775–5782.

[15] Y. Chen, G. Orosz, and T. G. Molnar, "Safe and stable connected cruise control for connected automated vehicles with response lag," *arXiv preprint arXiv:2409.06884*, 2024.

[16] Y. Chen, T. G. Molnar, and G. Orosz, "Feasible safe connected cruise control with backstepping control barrier functions," in *9th IEEE Conference on Control Technology and Applicat.*, 2025, pp. 590–595.

[17] X. Tan, W. S. Cortez, and D. V. Dimarogonas, "High-order barrier functions: Robustness, safety, and performance-critical control," *IEEE Transactions on Automatic Control*, vol. 67, no. 6, pp. 3021–3028, 2022.

[18] Y. Chen, T. G. Molnar, and G. Orosz, "Lag-compensating control barrier functions for feasible safety-critical control," in *American Control Conference*, 2026, accepted.

[19] M. Jankovic, "Robust control barrier functions for constrained stabilization of nonlinear systems," *Automatica*, vol. 96, pp. 359–367, 2018.

[20] I. Vörös, C. Jiang, H. Gan, D. Takács, X. Li, I. Kolmanovsky, J. Talbot, J. Dallas, J. Subosits, and G. Orosz, "Safe lane-keeping with control barrier functions: From theory to practical implementation," *IEEE Transactions on Control Systems Technology*, 2026, accepted.